DOI:10.28974/idojaras.2026.1.5

IDŐJÁRÁS

Quarterly Journal of the HungaroMet Hungarian Meteorological Service
Vol. 130, No. 1, January – March, 2026, pp. 87–100

Spatiotemporal trends in wood decay risk across European Russia (1961–2020): A Scheffer Climate Index analysis

Elena Vyshkvarkova[1,*] and **Olga Sukhonos**[2]

[1]*A.O. Kovalevsky Institute of Biology of the Southern Seas of RAS,*
299011, Nakhimov Avenue 2, Sevastopol, Russia

[2]*Institute of natural and technical systems,*
299011, Lenina St., 28, Sevastopol, Russia

**Corresponding author E-mail: aveiro_7@mail.ru*

(Manuscript received in final form June 10, 2025)

Abstract—This study evaluates the risk of wood decay in cultural heritage sites across the European part of Russia by analyzing climatic influences on timber deterioration. Timber, a critical component of many heritage structures, is particularly vulnerable to fluctuations in air temperature and moisture, which accelerate biological decay processes. Using the Scheffer Climate Index (*SCI*) – a metric based on average monthly temperature and the number of precipitation days –, the research assesses decay risk over the period 1961–2020 with daily data from the ERA5 reanalysis. The *SCI* was decomposed into temperature and precipitation components, and trends were quantified using the nonparametric Mann–Kendall test, with analyses performed for both the 1961–1990 and 1991–2020 periods. Results reveal a southwestward increase in *SCI* values, with the highest risks (*SCI* > 100) along the Black Sea coast and Caucasus. Notably, northern regions, home to key heritage sites like Kizhi Pogost, exhibited statistically significant upward *SCI* trends (up to 0.6/year), driven primarily by rising temperatures. Between 1961–1990 and 1991–2020, low-risk areas decreased by 9%, transitioning to moderate risk, while high-risk zones remained stable (~13%). Temperature contributions to *SCI* increased by 5–20%, whereas precipitation impacts declined, except in northern regions. Sequential analysis highlighted trend onset in the 2000s, particularly in the northwest and Caucasus. These findings underscore a rising climatic threat to wooden architectural heritage and emphasize the need for enhanced conservation strategies to mitigate future decay risks.

Key-words: cultural heritage sites, wood decay, Scheffer Climate Index, climate change

1. Introduction

Wooden architectural heritage constitutes a significant portion of cultural heritage sites worldwide, with many structures and their components crafted from this traditional building material. As an organic material, timber is particularly susceptible to environmental degradation, with its physical and mechanical properties deteriorating under various atmospheric influences (*Brimblecombe* and *Richards*, 2024). Among environmental factors, moisture and temperature fluctuations play the most critical role in the degradation processes of historical wooden structures (*Sabbioni et al.,* 2009, 2010; *Brimblecombe et al.,* 2011).

The hygroscopic nature of wood makes it vulnerable to damage caused by variations in atmospheric humidity, whether through excessive or insufficient moisture levels (*Blavier et al*., 2023; *Soboń* and *Bratasz,* 2022). Precipitation further exacerbates wood deterioration when water penetrates surface cracks and pores (*Blavier et al.,* 2023). Biological agents, including fungi, bacteria (*Koziróg et al*., 2016), and insects, pose additional threats, with decay fungi representing the most significant cause of economic losses in wooden heritage (*Brimblecombe* and *Lankester,* 2013; *Sesana et al*., 2021; *Prieto et al.,* 2020). Fungal activity depends critically on specific temperature and moisture conditions (*Curling* and *Ormondroyd*, 2020), while higher temperatures generally accelerate both biological degradation and insect infestation (*Flyen et al.,* 2020).

Photochemical degradation from ultraviolet and visible light leads to surface discoloration, increased moisture absorption, and enhanced biodegradation (*Andrady et al*., 2019). Additionally, atmospheric salts contribute to structural damage through crystallization processes and pore formation (*Mi et al*., 2020; *Wang et al.,* 2024).

Recent climatic changes have significantly impacted global hydrological cycles, with substantial precipitation variations observed since the mid-20th century (*IPCC,* 2021; *WMO,* 2021). These systemic climate changes present new challenges for cultural heritage preservation (*Sesana et al*., 2021; *Hall et al*., 2016). Numerous studies indicate that increasing atmospheric humidity, coupled with rising temperatures, creates favorable conditions for enhanced biological activity, accelerating the decomposition of wooden structures by fungi, mold, algae, and insects (*Sesana et al*., 2021; *Prieto et al*., 2020; *Camuffo*, 2019).

The Scheffer Climate Index (*Scheffer,* 1971) remains one of the earliest and most widely used tools for assessing climate-related risks to wood. Originally developed for the contiguous United States, this index estimates regional decay potential based on temperature and precipitation parameters. Subsequent applications have extended to Canada (*Wang* and *Morris,* 2008; *Morris* and *Wang*, 2011), Europe (*Fernandez-Golfin et al*., 2016; *Brimblecombe* and *Richards*, 2023a,b), Korea (*Oh et al*., 2022), and Africa (*Richards et al*., 2023).

The European part of Russia boasts numerous masterpieces of wooden architecture, including UNESCO World Heritage sites like the Kizhi Pogost (18th

century) in Karelia, the Malye Korely open-air museum in Arkhangelsk Oblast (featuring 400-year-old structures), and the Vitoslavlitsy museum in Novgorod Oblast. Other significant examples include the Kostroma Sloboda Museum reserve, historical buildings in Suzdal and Vologda, and architectural monuments throughout Leningrad, Nizhny Novgorod, Smolensk, and Tver regions.

This region exhibits substantial climatic diversity and has experienced significant warming trends (+0.55°C per decade) with variable precipitation patterns (*The Third Assessment Report*, 2022). These changing conditions differentially affect wooden structures across the region, necessitating detailed assessment. This study, therefore, aims to evaluate the potential risks of climate-induced degradation to wooden architectural heritage throughout European Russia, providing crucial data for conservation planning in the context of ongoing climate change.

2. Materials and methods

The daily data on air temperature and precipitation from the ERA5 reanalysis (spatial resolution 0.5°*0.5°) (*Hersbach et al*. 2020) for the period 1961–2020 for the European part of Russia were used. Data are freely available from the Copernicus Climate Data Store (*Copernicus Climate Change Service*). The study region is limited by coordinates 40°–65° N, 25°–50° E.

The analysis of the influence of climatic conditions on wooden heritage sites was carried out using the Scheffer index (*Scheffer,* 1971). The index selects two parameters (air temperature and precipitation) and helps to assess the risk of wood decay.

The Scheffer Climate Index (*SCI*) is calculated using the formula:

$$SCI = \frac{\sum_{Jan}^{Dec}[(T-2)(D-3)]}{16.7}, \quad (1)$$

where T is the average monthly temperature (°C) and D is the average number of days per month with precipitation greater than 0.3 mm per day (*Scheffer*, 1971; *Lisø et al*., 2006).

Months with average air temperatures below 2 °C and/or very little precipitation add nothing to the climate decay potential, as these conditions are not conducive to decay development. Moreover, the reduction that negative values of (T – 2) or (D – 3) introduce into the sum of Eq.(1) is irrelevant to the conceptual basis for developing the Scheffer index. Therefore, in the present study, the product (T − 2) × (D− 3) is always equal to or greater than zero (i.e., if (T − 2) or (D − 3) is negative for the i-th month of the year, then it is set equal to zero for that month) (*Nikolitsa* and *Giarma*, 2019; *Kim* and *Ra*, 2013; *Brischke* and *Selter*, 2020).

Additionally, the contribution of the temperature component (T_{SCI}) and the precipitation component (D_{SCI}) were calculated while maintaining the conversion factor of 16.7:

$$T_{SCI} = \sum_{Jan}^{Dec} [(T - 2)] / 16.7 \quad (2)$$

$$D_{SCI} = \sum_{Jan}^{Dec} [(D - 3)] / 16.7 \quad (3)$$

The overall risk is assessed based on the *SCI* values as follows: a value less than 35 indicates low risk, values from 35 to 65 indicate moderate risk, values from 65 to 100 indicate high risk, and values above 100 indicate very high risk (*Scheffer,* 1971).

The calculation results are presented as spatial maps for the reanalysis grid points to avoid distortions associated with data interpolation. Trends were calculated using the least squares method, and statistical significance was assessed using the nonparametric Mann-Kendall test with a statistical significance level of 0.05. For each period, the median value of the index was calculated for each grid point. The median was chosen because the values of the *SCI* are not characterized by a normal distribution (*Richards et al.,* 2023).

The sequential form of the non-parametric Mann-Kendall test was used as a method for analyzing progressive trends of the time series, which allows one to detect the approximate beginning of a developing trend (*Sneyers,* 1990). The sequential Mann-Kendall (*Moraes et al*., 1998) was used to test the start of a trend within the series *x1*, …, *xn*. The magnitudes of annual or seasonal mean time series *xj* (*j* = 1, …, *n*) were compared by *xk*(*k* = *1*, …, *j* − 1). For each comparison, the number of *xk* > *xj* was counted and denoted by *nj* (*Zhao et al.,* 2015). The test statistic was given as follows:

$$t_j = \sum_1^j n_j (j = 2,3, \dots, n) \quad (4)$$

$$E(t) = \frac{n(n-1)}{4} \quad (5)$$

$$Var(t_j) = \frac{j(j-1)(2j+5)}{72} \quad (6)$$

The sequential value of statistic *U(t)* which is the forward sequence was calculated as

$$U(t) = \frac{t_j - E(t)}{\sqrt{Var(t_j)}}, \quad (7)$$

where *u(t)* is a standardized variable with a zero mean and standard deviation equal to one, which fluctuates around zero as the time series progresses.

U'(t), which is the backward sequence, was calculated with the same formula with the reverse data time series.

The intersection of the curves *U(t)* and *U'(t)* indicates the year of the beginning of the trend, and the intersection point should be between the critical values of the confidence interval, i.e., between -1.96 and +1.96 (*Barbieri et al*., 2017; *Temeliyeh et al.,* 2022; *Chatterjee et al*., 2014). If *U(t)* exceeded the upper or lower 95 % confidence limits (+1.96 and −1.96 for an α=5 % significance level), there was a significant upward or downward trend in the time series (*Liu et al.,* 2008). The intersection of forward and backward curves of the test statistic detected the approximate time of occurrence of the trend (*Barbieri et al*. 2017). If the curves *U(t)* and *U'(t)* intersect in the critical range several times or U(t) crosses the confidence line several times, then there are no significant trends in the time series (*Dufek* and *Ambrizzi*, 2007; *Alijani et al.* 2011, *Temeliyeh et al*. 2022).

The results are obtained for the entire period (1961–2020), as well as for two sub-periods (1961–1990 and 1991–2020) which are defined by WMO as climate norms.

3. Results

3.1. Spatial distribution of the SCI values, temperature and precipitation components

The median values of the *SCI* in the study area in the period 1961–2020 vary within the range from 0 to 160 (*Fig. 1a*). The highest values (above 80) were found on the Black Sea coast of the Caucasus. Throughout the analyzed period, there was an increase in the index values from the northeast to the southwest. In the second climatic period (1991–2020), relative to the first period, there was an increase in the *SCI* across almost the entire analyzed area, especially pronounced in the northeast of the region (an increase of up to 100%) (*Fig. 1b*). The southern regions of the European part of Russia are characterized by a slight decrease in the *SCI* index to 20%, with the exception of the Caucasus ridge, where there is an increase in *SCI* by 80–90% in the highland part (*Fig. 1b*). The risk of wood decay under the influence of climatic factors increases in the southwest direction (*Fig. 1c*). Very high risk (*SCI* values above 100) was found for the Black Sea coast of the Caucasus, Ciscaucasia, and Transcaucasia.

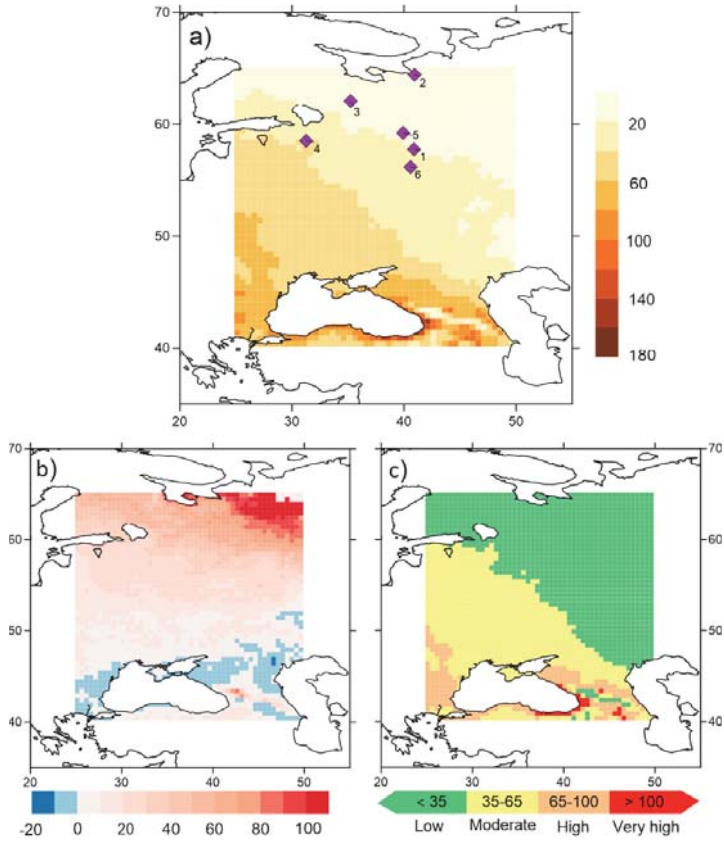

Fig. 1. Spatial distribution of (a) median values of the *SCI* for the entire period (1961–2020); (b) the difference (in %) of the index between the two sub-periods (1961–1990 and 1991–2020); (c) wood decay risk for the period 1961–2020. The diamonds in (a) correspond to the main sites of wooden architecture: *1* –Kostroma Sloboda Museum reserve, *2* –Malye Korely open-air museum in Arkhangelsk Oblast, *3* – Kizhi Pogost, *4* –Vitoslavlitsy museum in Novgorod Oblast, *5* and *6* – historical buildings in Suzdal and Vologda.

The presentation of the results in gradations of the *SCI* values shows that in the second climatic period (1991–2020), compared to the first period, there was a decrease (by 9%) in the area of the territory with a low risk of wood decay, due to an increase in the area with a moderate risk (from 34% to 43%). In the period 1991–2020, the areas of the territory with low and moderate risks become almost equal. The area with a high risk did not change between the two climatic norms and is about 13%.

The *SCI* includes two components: temperature and precipitation. Spatial maps of these components are shown in *Fig. 2*. The entire study area is characterized by an increase in the contribution of the temperature component to

the *SCI*. The change (growth) of the temperature component between the two subperiods in most of the study region is 5–15%. The maximum increase in the contribution of the temperature component to the *SCI* in the second climatic period was found for the territory of Lake Onega (location of the UNESCO cultural heritage site Kizhi Pogost) up to 20%. The opposite picture is observed for the precipitation component. Almost the entire territory shows a decrease in the contribution of precipitation to 15% in the second climatic period compared to the first. A slight increase in the contribution of precipitation (up to 5%) to the *SCI* is observed in the northern regions.

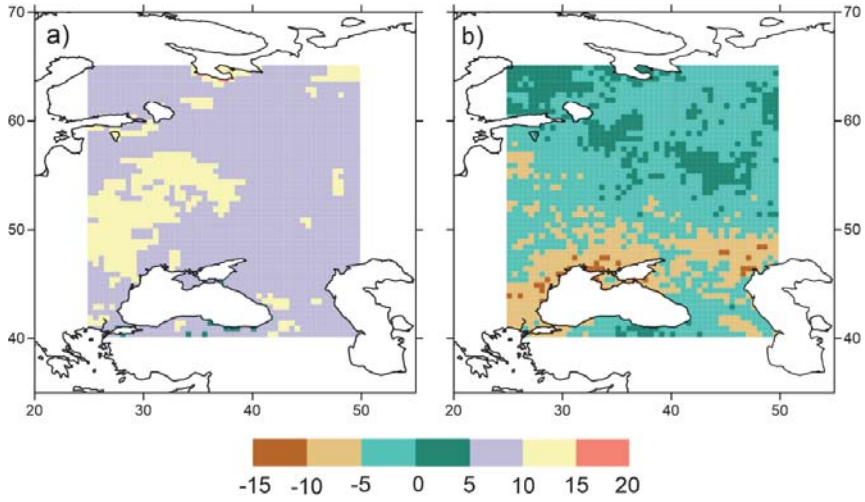

Fig. 2. Change (in %) in the contribution of the temperature (a) and precipitation (b) components of the *SCI* between two periods 1991–2020 and 1961–1990

3.2. Trends of SCI, temperature, and precipitation components

The *SCI* trends for the period 1961–2020 are predominantly positive in the study area. North of 50 degrees latitude, the trend values are statistically significant. The maximum trend values reach 0.6/year in the northwest of the region (*Fig. 3*). The Ciscaucasia is characterized by negative, but statistically insignificant trends, while the Caucasus Mountains itself has a positive *SCI* trend with values from 0.2 to 0.4/year for the period 1961–2020. The trends in the temperature component of the *SCI* are positive and statistically significant throughout the region, with the highest trend values on the northwest coast of the Black Sea and in the White Sea

area. Negative statistically significant trends in the precipitation component of the *SCI* are typical for the northern Black Sea region, the Caucasus Mountains, and the western coast of the Black Sea (*Sukhonos et al*., 2024).

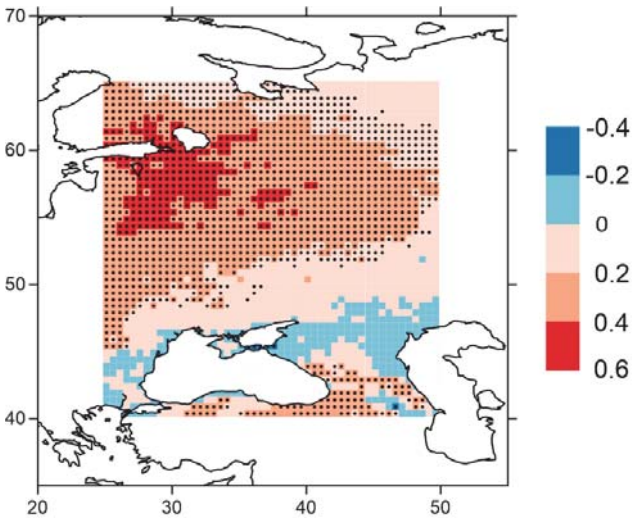

Fig. 3. Trends of the *SCI* for the period 1961–2020. Black dots are statistically significant trends ($p<0.05$)

Using the Mann-Kendall sequential test, estimates of the approximate date of the onset of a significant trend in the *SCI* are obtained. The *Fig. 4* shows spatial maps of statistically significant ($p<0.05$) intersection of the *U(t)* and *U'(t)* curves for the entire period 1961–2020. As it can be seen, the *SCI* index is characterized by upward trends in the northwestern areas of the study region and in the Caucasus Mountains. Single downward trends are found in the Ciscaucasia on the Caspian Sea coast. The temperature component of the *SCI* has upward trends throughout almost the entire territory of the study region for the period 1961–2020, with the exception of the Caucasus Mountains. The precipitation component is characterized by a small number of reanalysis grid points with statistically significant downward trends in the central regions and the Ciscaucasia.

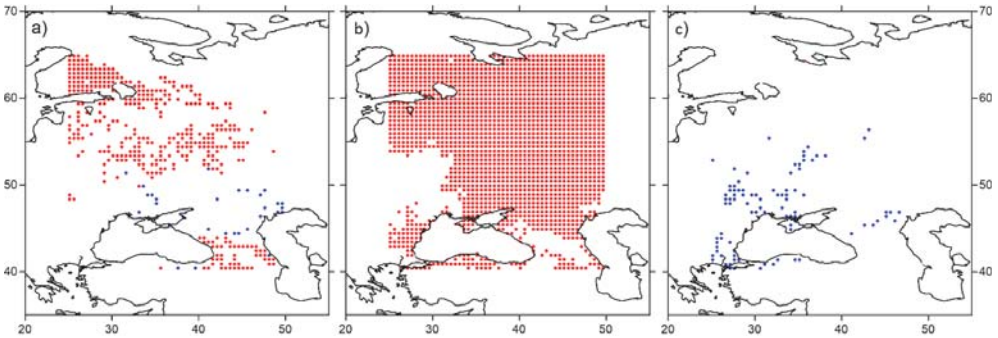

Fig. 4. Spatial distribution of grid points with statistically significant intersection of the *U(t)* and *U'(t)* curves ($p<0.05$) for the period 1961–2020 for *SCI* (a), temperature component (b), and precipitation component (c).

The percentage of grid points with trends of opposite signs is presented in *Table 1*. The maps presented in *Fig. 4* show the total number of statistically significant intersections of the *U(t)* and *U'(t)* curves for the entire period. The distribution by years of the number of grid points with the total number of intersections of the *U(t)* and *U'(t)* curves and the statistically significant ones for the period 1961–2020 are presented in *Fig. 5a*. In some years, the percentage of grid points with intersections reaches 5.3% (1980), while the percentage of significant intersections reaches approximately 2.5% in the same 1980 and in 2003. When comparing the two subperiods, it is clear that the number of intersections of the *U(t)* and *U'(t)* curves in the first period 1961–1990 is higher compared to the second period, but the percentage of statistically significant transitions increases in the second period. The largest number of statistically significant intersections of the curves *U(t)* and *U'(t)* occurs in the 2000s. The spatial distribution of grid points with statistically significant intersections of the *U(t)* and *U'(t)* curves related to the two sub-periods (*Fig. 5b*) shows that in the first period (1961–1990), grid points are concentrated in the central region of the study region, while in the second period (1991–2020), statistically significant intersections are localized in the Caucasus Mountains and in the northwest of the region (*Fig. 5b*).

Table 1. Percentage of grid points with significant intersections ($p<0.05$) of the *U(t)* and *U'(t)* curves

Indicator	Number of grid points (%)		
	total quantity	upward	downward
SCI	16.84	15.48	1.36
T_{SCI}	72.80	72.80	0.00
D_{SCI}	3.64	0.00	3.64

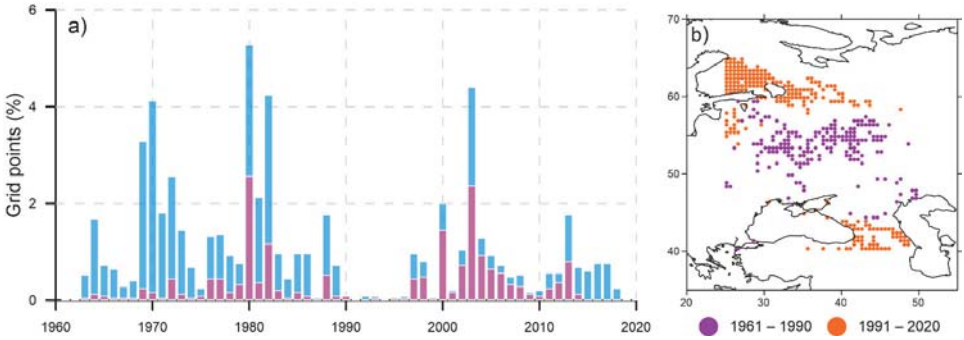

Fig. 5. (a) Percentage of grid points (blue bars) that intersect in each year and are statistically significant at the 95% level intersection (brown bars) of the *SCI*; (b) distribution of significant intersections of the curves *U(t)* and *U'(t)* for the *SCI* index, related to two periods without taking into account the sign of the trend.

4. Discussion and conclusions

Using the Scheffer Climate Index and the data from ERA5 re-analysis, the risk of wood decay of cultural heritage sites in the European part of Russia was assessed for the period 1961–2020. The risk of wood decay increases in the southern direction, the maximum values of the *SCI* were found for the Black Sea coast of the Caucasus, the Ciscaucasia, and Transcaucasia. Masterpieces of wooden architecture in the European part of Russia are located mainly in its northern regions, where the largest values of statistically significant trends of *SCI* were found. Previously, statistically significant trends in the number of freeze-thaw cycles and the number of days with relative air humidity over 80% for the same time period were obtained for the northern regions of the European part of Russia (*Vyshkvarkova* and *Sukhonos,* 2023).

A positive trend in the *SCI* values, and the resulting increase in the risk of wood decay, is found elsewhere in other studies. An increase in the *SCI* values, temperature and precipitation components, from 1900 to 2020 with varying intensity was found for three stations in Russia (St. Petersburg, Arkhangelsk, and Shenkursk in the Arkhangelsk region) (B*rimblecombe* and *Richards*, 2023a). There has been a significant increase in *SCI* for locations across the UK between 1990 and 2019. The highest values are found in the northern and western parts of the UK, but increases have been seen across the country (*Curling* and *Ormondroyd*, 2020).

Positive trends in the *SCI* values are expected to continue in the future, according to regional and global climate models in different regions of the globe. For example, the results of the global HadGEM3 model predict an increase in the

SCI values from 50 (1850–1879) to 75 (2070–2099) across Europe (*Richards* and *Brimblecombe*, 2022). In the coming years, an increase in the risk of wood decay can be expected in the Trentino-South Tyrol region, according to the CORDEX model ensemble for RCP4.5 and RCP8.5 scenarios (*Blavier et al*., 2024). For Africa, 13 CMIP6 models and the SPS585 scenario found that projections of future changes in the *SCI* are driven primarily by changes in temperature rather than precipitation. Despite significant disagreement in the simulated magnitude of the *SCI*, there was good agreement between models on the direction of change in Equatorial Africa, where the *SCI* is highest (*Richards et al*., 2023). Results from the HadGEM3-RA model under the RCP4.5 and 8.5 scenarios for Korea show that climate change will significantly increase the potential decay risk and, as a result, the vulnerability of wooden cultural heritage to fungal decay by the end of the century, even under the RCP 4.5 scenario (*Oh et al.,* 2022). Based on meteorological station data, the risk of wood decay for Iran is assessed as low in most areas and moderate in the northern part of the country along the Caspian Sea coast (*Helali et al*., 2021). Using long-term observational data (since the late 19th century), the authors (*Brimblecombe* and *Richards*, 2023b) assessed the past and future change in the *SCI* for Europe and concluded that the threat to wood heritage is increasing in temperate and continental regions of Europe, and decreasing along the northern Mediterranean coast. *Vandemeulebroucke et al*. (2021) showed the increase in mould and wood decay under RCPs 4.5 and 8.5 scenarios by the end of the 21st century using a solid masonry case study in Brussels, Belgium.

The use of sequential Mann-Kendall test allowed to establish some patterns of change in the sign of the *SCI* index trend. The two identified sub-periods have differences in the spatial distribution of upward and downward trends. The first period is characterized by a statistically significant change in the sign of the trend in the central regions, while in the second period, the areas of statistically significant intersections of the curves are in the northwest of the region and in the Caucasus Mountains.

Our results are consistent with those of other studies and show an increase in the risk of decay of wood of cultural heritage sites in many regions of the globe against the background of observed climate change. The northern regions of the European part of Russia, despite moderate values of the *SCI*, have the greatest positive trend, which indicates an increasing threat to wooden structures. Intensification of measures to support and protect cultural heritage sites consisting of wood or having wood components is required.

Funding. This work was supported by the state assignment of Institute of Natural and Technical Systems (Project Reg. No. 124013000609-2).

References

Alijani, B., Mahmoudi, P., Salighe, M., and *Rigi, A*., 2011: Study of annual maximum and minimum temperatures Changes in Iran. *Geograp. Res. 26,* 101–122.

Andrady, A.L., Pandey, K.K., and *Heikkilä, A.M.*, 2019: Interactive effects of solar UV radiation and climate change on material damage. *Photochem. Photobiol. Sci. 18,* 804–825. https://doi.org/10.1039/c8pp90065e

Barbieri, L.F.P., Correia, M. de F., Aragão, M.R. da S., Vilar, R.A.A,. and *de Moura, M.S.B.*, 2017: Impact of climate variations and land use change: A Mann-Kendall Application. *Rev Geama Recife 3(3),* 127–135.

Blavier, C.L.S., Huerto-Cardenas, H.E., Aste, N., Del Pero, C., Leonforte, F., Della, and *Torre, S.*, 2023: Adaptive measures for preserving heritage buildings in the face of climate change: A review. *Building and Environment 245*, e110832. https://doi.org/10.1016/j.buildenv.2023.110832

Blavier, C.L.S., Maines, E., Campalani, P., Huerto-Cardenas, H.E., Del Pero, C., and *Leonforte, F*., 2024: Assessing Climate Impact on Heritage Buildings in Trentino-South Tyrol: High-Resolution Projections and Adaptive Strategies. Preprint. https://doi.org/10.2139/ssrn.4985301

Brimblecombe, P., Grossi, C.M., Harris, I., 2011: *Climate change critical to cultural heritage*. In: Gökçekus H, Türker U, LaMoreaux JW (eds) Survival and sustainability: environmental concerns in the 21st century, Springer, 195–205

Brimblecombe, P., Lankester, P., 2013: Long-term changes in climate and insect damage in historic houses. *Studies in Conservation 58*, 13–22. https://doi.org/10.1179/2047058412Y.0000000051

Brimblecombe, P. and *Richards, J.,* 2023a: Köppen climates and Scheffer index as indicators of timber risk in Europe (1901–2020). *Heritage Science 11*, 148. https://doi.org/10.1186/s40494-023-00992-7

Brimblecombe, P. and *Richards, J.,* 2023b: Temporal resolution of climate pressures on façades in Oxford 1815–2021. *Theor. Appl. Climatol. 153*, 561–572. https://doi.org/10.1007/s00704-023-04498-x

Brimblecombe, P., Richards, J., 2024: Applied climatology for heritage. *Theor. Appl. Climatol. 155*, 7325–7333. https://doi.org/10.1007/s00704-024-05059-6

Brischke, C. and *Selter, V.,* 2020: Mapping the decay hazard of wooden structures in topographically divergent regions. *Forests 11(5)*, e510. https://doi.org/10.3390/f11050510

Camuffo, D., 2019: Climate change, human factor, and risk assessment. In: *D. Camuffo*, ed., Microclimate for cultural heritage, Elsevier, 303–340.

Chatterjee, S., Bisai, D., and *Khan, A*., 2014: Detection of approximate potential trend turning points in temperature time series (1941–2010) for Asansol Weather Observation Station, West Bengal, India. India. *Atmosp. Climate Sci. 4*, 64–69.

Copernicus Climate Change Service. Access to ERA5 Reanalysis Data. Available at: https://climate.copernicus.eu/climate-reanalysis [Accessed on 24 December 2024].

Curling, S.F. and *Ormondroyd, G.A*., 2020: Observed and projected changes in the climate based decay hazard of timber in the United Kingdom. *Scientific Reports 10*, e16287. https://doi.org/10.1038/s41598-020-73239-1

Dufek, A.S. and *Ambrizzi, T*., 2008: Precipitation variability in São Paulo State, Brazil. *Theor. Appl. Climatol. 93*, 67–178. https://doi.org/10.1007/s00704-007-0348-7

Fernandez-Golfin, J., Larrumbide, E., Ruano, A., Galvan, J., and *Conde, M*., 2016: Wood decay hazard in Spain using the Scheffer index: proposal for an improvement. *Eur J Wood Wood Prod 74*, 591–599.

Flyen, A.-C., Flyen, C., and *Mattsson, J*., 2020: Climate change impacts and fungal decay in vulnerable historic structures at Svalbard. *E3S Web Conf 172*, e20006. https://doi.org/10.1051/e3sconf/202017220006

Hall, C.M., Baird, T., James, M., Ram, Y., 2016: Climate change and cultural heritage: conservation and heritage tourism in the Anthropocene. *J. Heritage Tourism 11*, 10–24. https://doi.org/10.1080/1743873X.2015.1082573

Helali, J., Momenzadeh, H., Saeidi, V., Brischke, C., Ebrahimi, G., and *Lotfi, M.,* 2021: Decadal Variations of Wood Decay Hazard and El Niño Southern Oscillation Phases in Iran. *Front For Glob Change 4*, 693833. https://doi.org/10.3389/ffgc.2021.693833

Hersbach, H., Bell, B., Berrisford, P., Hirahara, S., Horanyi, A., Muñoz-Sabater, J., Nicolas, J., Peubey, C., Radu, R., Schepers, D., Simmons, A., Soci, C., Abdalla, S., Abellan, X., Balsamo, G., Bechtold, P., Biavati, G., Bidlot, J., Bonavita, M., De Chiara, G., Dahlgren, P., Dee, D., Diamantakis, M., Dragani, R., Flemming, J., Forbes, R., Fuentes, M., Geer, A., Haimberger, L., Healy, S., Hogan, R.J., Hólm, E., Janisková, M., Keeley, S., Laloyaux, P., Lopez, P., Lupu, C., Radnoti, G., de Rosnay, P., Rozum, I., Vamborg, F., Villaume, S., and *Thépaut, J.-N.*, 2020: The ERA5 global reanalysis. *Q. J. R. Meteorol. Soc. 146*, 1999–2049. https://doi.org/10.1002/qj.3803

IPCC 2021: Climate Change 2021: The Physical Science Basis. Contribution of Working Group I to the Sixth Assessment Report of the Intergovernmental Panel on Climate Change. In: *Masson-Delmotte, V., Zhai, P., Pirani, A., Connors, S.L., Péan, C., Berger, S., Caud, N., Chen, Y., Goldfarb, L., Gomis, M.I., Huang, M., Leitzell, K., Lonnoy, E., Matthews, J.B.R., Maycock, T.K., Waterfield, T., Yelekçi, O., Yu, R., Zhou, B.* (eds) Cambridge University Press, 3949 p. https://www.ipcc.ch/report/ar6/wg1/downloads/report/IPCC_AR6_WGI_Full_Report.pdf

Kim, T. and *Ra, J.B.,* 2013: Decay hazard (Scheffer) index values in Korea for exterior aboveground wood. *Forest Products Journal 63 (3-4)*, 91–94.

Koziróg, A., Rajkowska, K., Otlewska, A., Piotrowska, M., Kunicka-Styczynska, A., Brycki, B., Nowicka-Krawczyk, P., Koscielniak, M., and *Gutarowska, B.*, 2016: Protection of Historical Wood against Microbial Degradation – Selection and Application of Microbiocides. *Int. J. Mol. Sci. 17*, e1364. https://doi.org/10.3390/ijms17081364

Lisø, K.R., Hygen, H.O., Kvande, T., and *Thue, J.V.*, 2006: Decay potential in wood structures using climate data. *Build Res Inf 34*, 546–551.

Liu, Q., Yang, Z., and *Cui, B.,* 2008: Spatial and temporal variability of annual precipitation during 1961–2006 in Yellow River Basin, China. *J. Hydrol.361*, 330–338.

Mi, X., Li, T., Wang, J., and *Hu, Y.,* 2020: Evaluation of salt-induced damage to aged wood of historical wooden buildings. *Int. J. Anal. Chem*. e8873713. https://doi.org/10.1155/2020/8873713

Moraes, J.M., Pellegrino, H.Q., Ballester, M.V., Martinelli, L.A., Victoria, R.L., and *Krusche, A.V.,* 1998: Trends in hydrological parameters of southern Brazilian watershed and its relation to human induced changes. *Water Resour. Manage. 12*, 295–311.

Morris, P.I. and *Wang, J.*, 2011: Scheffer index as preferred method to define decay risk zones for above ground wood in building codes*. International Wood Products J. 2*, 67–70. https://doi.org/10.1179/2042645311Y.0000000012

Nikolitsa, G. and *Giarma, C.*, 2019: Estimation of decay potential of wooden elements above ground in Greece. *Build. Environ. 154*, 155–166

Oh, J.-J., Choi, Y.-S. sun Kim, G., and *Kim, G.-H.*, 2022: Assessment of the effects of projected climate change on the potential risk of wood decay in Korea. *J. Cultural Heritage 55*, 43–47. https://doi.org/10.1016/j.culher.2022.02.004

Prieto, B., Vazquez-Nion, D., Fuentes, E., and *Duran-Roman, A.G.*, 2020: Response of subaerial biofilms growing on stone-built cultural heritage to changing water regime and CO2 conditions. *Int. Biodeteriorat. Biodegradat. 148*, e104882. https://doi.org/10.1016/j.ibiod.2019.104882

Richards, J. and *Brimblecombe, P.*, 2022: Moisture as a driver of long-term threats to timber heritage—Part I: changing heritage climatology. *Heritage 5*, 1929–1946. https://doi.org/10.3390/heritage5030100

Richards, J., Brimblecombe, P., and *Engelstaedter, S.*, 2023: Modelling temperature-precipitation pressures on African timber heritage. *Int. J. Climatol. 43(16)*, 7447–7462. https://doi.org/10.1002/joc.8273

Sabbioni, C., Brimblecombe, P., and *Cassar, M.*, 2010: The atlas of climate change impact on European cultural heritage. Scientific analysis and management strategies. London: Anthem Press.

Sabbioni, C., Cassar, M., Brimblecombe, P., 2009: Vulnerability of cultural heritage to climate change. *Pollution Atmospherique 203*, 285–298

Scheffer, T.C., 1971: A climate index for estimating potential for decay in wood structures above ground. *Forest Products Journal 21*, 25–31.

Sesana, E., Gagnon, A.S., Ciantelli, C., Cassar, J.A., and *Hughes, J.J*., 2021: Climate change impacts on cultural heritage: A literature review. *WIREs Clim Change 12*, e710. https://doi.org/10.1002/wcc.710

Sneyres, R., 1990: Technical note no. 143 on the statistical analysis of time series of observation World Meteorological Organization, Geneva, Switzerland.

Soboń, M. and *Bratasz, Ł*., 2022: A method for risk of fracture analysis in massive wooden cultural heritage objects due to dynamic environmental variations. *Eur J Wood Prod 80*, 1201–1213. https://doi.org/10.1007/s00107-022-01841-3

Sukhonos, O.Yu., Vyshkvarkova, E.V., and *Voskresenskaya, E.N*., 2024: Trends in the Sheffer index as an indicator of the risk of destruction of wooden structures of cultural heritage sites in the European part of Russia. *Environ. Control Syst. 4,* 115–122. (in Russian). https://doi.org/10.33075/2220-5861-2024-4-115-122

Temeliyeh, Z.K., Temeliyeh, S.K., Temeliyeh, H.K., and *Mirabbasi, R*., 2022: Investigating the Trend of Temperature Changes in Isfahan Station, Iran Using the Sequential Mann-Kendall Method. *Water Harvesting Research 5(2*), 217–228. https://doi.org/10.22077/jwhr.2023.6429.1086

The Third Assessment Report on Climate Change and its Consequences in the Russian Federation, 2022: Kattsov, V.M. (ed) Roshydromet, St. Petersburg: Science-Intensive Technologies, 676 p

Vandemeulebroucke, I., Caluwaerts, S., and *Van Den Bossche, N.,* 2021: Factorial Study on the Impact of Climate Change on Freeze-Thaw Damage, Mould Growth and Wood Decay in Solid Masonry Walls in Brussels. *Buildings 11*, e134. https://doi.org/10.3390/buildings11030134

Vyshkvarkova, E., Sukhonos, O., 2023: Climate Change Impact on the Cultural Heritage Sites in the European Part of Russia over the Past 60 Years. *Climate 11*, e50. https://doi.org/10.3390/cli11030050

Wang, F., Huang, J., and *Zhou, Q*., 2024: Water-salt transport modeling and sulfate erosion mechanisms in cultural heritage under microclimate. *J. Build Engin 98*, e111393. https://doi.org/10.1016/j.jobe.2024.111393

Wang, J. and *Morris, P*., 2008: Effect of Climate change on above ground decay hazard for wood products according to the Scheffer index. Proceedings of the 29th Canadian Wood Preservers Association Annual Meeting Vancouver 2008, 92–103. https ://www.cwpa.ca/publi catio ns/#tab-2008-tab

WMO, 2021: State of the Global Climate 2020 – WMO, 1264, 56 p. https://library.wmo.int/doc_num.php?explnum_id=10618

Zhao, J., Huang, Q., Chang, J., Liu, D., Huang, S., and *Shi, X*., 2015: Analysis of temporal and spatial trends of hydro-climatic variables in the Wei River Basin. *Environ. Res. 139*, 55–64. https://doi.org/10.1016/j.envres.2014.12.028